Asian Journal of Applied Research for Community Development and Empowerment. Vol 9 (2025), No.3

e-ISSN 2581-0405

ajarcde

Asian Journal of Applied Research for Community Development and Empowerment

Journal home page: http://ajarcde-safe-network.org   ISSN 2581-0405

# Efficiency of Fly Ash and Corncob as Alternative Adsorbents for Reducing $Fe^{2+}$ and $Mn^{2+}$ in Groundwater

*Lucia Adelina Devitasari*[1] *and Mohamad Mirwan* [2]

[1,2] *Department of Environmental Engineering, Faculty of Engineering and Science, Universitas Pembangunan Nasional "Veteran" Jawa Timur, Surabaya, Indonesia*

**ARTICLE INFO**

*Article History:*
Received: 01 November 2025
Final Revision: 18 November 2025
Accepted: 20 November 2025
Online Publication: 21 November 2025

**KEYWORDS**

*Adsorption, Alternative Adsorbent, Fly Ash, Corncob, Dissolved Iron, Dissolved Manganese*

**CORRESPONDING AUTHOR**

*E-mail: mmirwan.tl@upnjatim.ac.id

## ABSTRACT

Groundwater quality deterioration is common in densely populated areas and industrial zones due to elevated levels of $Fe^{2+}$ and $Mn^{2+}$, which alter water's physical properties and pose potential health risks. This study aimed to evaluate the efficacy of fly ash and corn cob as alternative adsorbents for reducing $Fe^{2+}$ and $Mn^{2+}$ concentrations in groundwater through continuous adsorption processes, with variations in adsorbent bed height and sampling time using 40% $H_3PO_4$ as an activator. The results demonstrated that both fly ash and corn cob were effective, achieving optimum removal efficiencies of 99.7% for $Fe^{2+}$ and 89.2% for $Mn^{2+}$ using fly ash, and 99.2% for $Fe^{2+}$ and 87.7% for $Mn^{2+}$ using corn cob. Increasing the adsorbent bed height and extending sampling time enhanced the removal efficiency of $Fe^{2+}$ and $Mn^{2+}$. FTIR analysis confirmed the involvement of –OH, Si–O, C=O, and C–O functional groups in the adsorption process. The Thomas model indicated that $Q_0$ decreased while $K_T$ increased with increasing adsorbent height. Corn cob exhibited a higher adsorption capacity, whereas fly ash demonstrated faster kinetic rates, with $R^2$ values ranging from 0.8052 to 0.9807.

### Contribution to Sustainable Development Goals (SDGs):

**SDG 6:** Clean Water and Sanitation
**SDG 12:** Responsible Consumption and Production

## 1. INTRODUCTION

### *1.1. Research Background*

Groundwater serves as one of the primary sources of clean water for communities. However, its quality in several regions of Indonesia, particularly in areas characterized by intensive industrial activities and high-density settlements, often fails to meet regulatory standards. One of the major contaminants is elevated dissolved metal concentrations, especially iron (Fe) and manganese (Mn). According to the Indonesian Ministry of Health Regulation 2/2023, the maximum allowable levels of Fe and Mn in clean water are 0.2 mg/L and 0.1 mg/L, respectively. Previous research by [1] Reported Fe levels of 9.667 mg/L and Mn levels of 1.74 mg/L, both of which exceed the established thresholds. These elevated levels not only degrade the physical quality of groundwater but also pose potential risks to public health. The presence of these metals contributes to undesirable changes in water odour and colour, as well as sediment formation, and may lead to various health concerns.

Adsorption is recognized as an effective and environmentally sustainable method for reducing dissolved metal concentrations, owing to its simplicity, cost-effectiveness, and high removal efficiency. [2]. This process employs porous materials (adsorbents) to capture contaminants from water onto solid surfaces. Adsorbents may be synthetic, natural, or derived from waste materials (bio-adsorbents). Low-cost, waste-based adsorbents such as fly ash and corncob provide a sustainable alternative while supporting circular-economy principles.

Fly ash, generated as a solid residue from coal combustion, is rich in silica ($SiO_2$) and alumina ($Al_2O_3$). These components provide numerous active sites that facilitate adsorption. [3]. In contrast, corncob biomass consists of cellulose and hemicellulose, with functional groups such as –OH, –COOH, and $–NH_2$ that can bind metal ions. The pore structure and surface chemistry of both materials can further enhance their adsorption capacity, particularly upon chemical activation with acidic or basic agents. Their porous nature and active functional groups make fly ash and corncob promising candidates for the reduction of $Fe^{2+}$ and $Mn^{2+}$ concentrations in groundwater.

## 1.2. *Literature Review*

### *1.2.1. Adsorption*

Adsorption refers to the process in which dissolved species (adsorbates) adhere to the surface of a solid phase (adsorbent), causing their concentration in the solution to decline. This mechanism typically occurs through three main steps. The first is film diffusion, in which the adsorbate moves across a thin boundary layer that envelops the adsorbent. This is followed by pore diffusion, where the molecules enter and travel through the adsorbent's internal pore structure. The final step involves surface interaction, during which the molecules adhere to the surface through physical or chemical bonding mechanisms [4].

Based on the nature of the interactions involved, adsorption can be classified into physisorption and chemisorption. Weak Van der Waals forces control physisorption, which occurs reversibly and is favoured at lower temperatures and higher pressures because reduced kinetic energy facilitates the adherence of molecules to the surface [5]. In contrast, chemical adsorption involves the formation of strong chemical bonds, such as covalent bonds, and is irreversible; it typically requires surface activation through chemical treatment [6].

### *1.2.2. Fly Ash*

Fly ash is a fine particulate material produced from coal combustion and captured from flue gas using electrostatic precipitators or baghouse filters. Its chemical composition is dominated by silica, alumina, iron oxide, and calcium oxide, with their relative abundances subject to variation based on the coal origin [7] . Its small particle size and relatively large surface area give fly ash reactive characteristics and make it suitable for use as an adsorbent [8].

The adsorption performance of fly ash is influenced by its metal oxide content and porous structure, which enable the uptake of dissolved ions through surface interactions. Studies have shown that fly ash is effective in removing heavy metals from aqueous solutions. Chemical activation or thermal treatment can enhance its surface area and improve its adsorption capacity [9].

### *1.2.3. Corncob*

Corncob is an abundant agricultural by-product with a high carbon content (±43%), making it suitable for conversion into activated carbon as an adsorbent [10]. Its chemical composition, dominated by cellulose, hemicellulose, and lignin, plays a crucial role in enabling effective carbonization and fostering the development of a well-defined porous structure. [11].

Functionally, corncob contains polar groups such as –OH and –COOH, enabling ion-exchange and hydrogen-bonding mechanisms during adsorption. Its macroporous structure enhances ion diffusion and increases adsorption rates. [12]. XRF characterization indicates that light-brown corncob ash has metal oxide compositions more suitable for adsorption applications [13].

### *1.2.4. Factor Influencing Adsorption*

Several key factors govern adsorption efficiency. Contact time determines the duration of interaction between the adsorbent and adsorbate. Increasing contact time generally enhances adsorption until equilibrium is reached, although excessively long contact may lead to desorption. The amount of adsorbent and agitation also accelerates equilibrium by increasing the frequency of molecular collisions. [13].

Adsorbent characteristics, including moisture content, ash content, particle size, and pore structure, play a critical role in determining adsorption capacity. Low moisture and ash levels help maintain porosity and surface area. Smaller particles provide a larger surface area and thus higher adsorption efficiency, while appropriate pore sizes allow adsorbate molecules to enter and interact effectively. However, excessive adsorbent dosage may reduce efficiency because not all surfaces can interact with the solution. [14].

### *1.2.5. Thomas Kinetic Model*

The Thomas model assumes that the adsorption rate follows first-order kinetics with respect to solute concentration and the accessible reactive sites on the adsorbent. It further provides a linearised expression relating the influent concentration ($C_0$) to the effluent concentration ($C_e$) at a given time.

$$\mathrm{Ln}\left(\frac{\mathrm{Co}}{\mathrm{Ce}} - 1\right) = \mathrm{K_T}.\mathrm{Qo}.\frac{\mathrm{m}}{\mathrm{Q}} - \mathrm{K_T}.\mathrm{Co}.\mathrm{t} \tag{1}$$

The model yields two primary parameters: $K_T$, representing the adsorption rate constant, and $Q_0$, which reflects the maximum adsorption capacity. These parameters are used to describe column dynamics and to predict the breakthrough curve. Due to its ability to accurately and practically represent adsorption behaviour, the Thomas model is extensively applied to estimate the actual adsorption capacity in continuous-flow systems. [15].

## 1.3. *Research Objective*

This study analyses the effectiveness of fly ash and corncob as alternative adsorbents for reducing $Fe^{2+}$ and $Mn^{2+}$ concentrations in groundwater via continuous adsorption. In addition, the study identifies changes in active functional groups using FTIR analysis and determines adsorption capacity through the application of the Thomas kinetic model.

# 2. MATERIALS AND METHODS

## 2.1. *Equipment and Materials*

This study employed several instruments to support the experimental procedures, including a furnace, an oven, 100–150 mesh sieves, and 200–300 mesh sieves. The materials used in this research included corncob biomass, fly ash, distilled water, a 40% $H_3PO_4$ activating solution, and groundwater samples.

### 2.2. *Preparation and Activation of Corncob-Based Activated Carbon*

The corncobs were first washed, chopped into smaller pieces, and dried in sunlight. After drying, they were carbonized at 400 °C for 1 hour. The produced char was then ground and sieved to obtain a particle size of 200–300 mesh. This carbon material was further activated by soaking it in a 40% $H_3PO_4$ solution for 24 hours, followed by thorough washing until the pH was neutral, and finally dried at 120 °C for 2 hours.

### 2.3. *Preparation and Activation of Fly Ash-Based Activated Carbon*

The fly ash was initially weighed, rinsed with distilled water, and oven-dried at 90 °C for one hour. It was then chemically activated by immersion in a 40% $H_3PO_4$ solution for 24 hours. After activation, it was washed until reaching neutral pH and subsequently dried at 120 °C for two hours. The dried product was finally milled and sieved to obtain particles in the 100–150 mesh range.

### 2.4. *Adsorption of $Fe^{2+}$ and $Mn^{2+}$*

The adsorption process was carried out in a continuous system. Groundwater from the feed tank was pumped to an initial holding tank, then flowed through the adsorption column, and finally was directed to the effluent tank. Sampling in the adsorption column was performed based on variations in adsorbent bed height (10, 20, 30, 40, and 50 cm), sampling times (45, 60, 75, 90, 105, and 120 minutes), and adsorbent types (fly ash and corncob). The treated water samples were subsequently analyzed to determine the concentrations of dissolved metal ions ($Fe^{2+}$ and $Mn^{2+}$).

## 3. RESULT AND DISCUSSION

### 3.1. *Groundwater Characteristics*

The groundwater sample was collected from Kras District, Kediri Regency, East Java, an area located near an industrial zone and potentially exposed to pollution. Laboratory testing indicated that the $Fe^{2+}$ concentration was 1.305 mg/L and the $Mn^{2+}$ concentration was 2.96 mg/L, both of which surpass the limits set by the Indonesian Ministry of Health Regulation 2/2023, which requires $Fe^{2+}$ levels to be under 0.2 mg/L and $Mn^{2+}$ levels to be below 0.1 mg/L. Elevated $Fe^{2+}$ levels can cause a metallic taste, brownish colouration, and corrosion of household appliances, while excessive $Mn^{2+}$ levels can lead to black deposits and pose risks to the human nervous system.

### 3.2. *Efficiency of Alternative Adsorbents using Fly Ash and Corncob*

The reduction of $Fe^{2+}$ and $Mn^{2+}$ concentrations in groundwater containing dissolved metal ions exhibited varying levels of efficiency throughout the adsorption process. This study employed two alternative adsorbents, fly ash and corncob, each possessing distinct adsorption characteristics. The efficiency of $Fe^{2+}$ and $Mn^{2+}$ removal from groundwater using fly ash is presented in Table 1.

**Table 1**. Reduction of $Fe^{2+}$ and $Mn^{2+}$ using Fly Ash as an Alternative Adsorbent

| Adsorbent Height (cm) | Sampling Time (Minutes) | Reduction in Concentration (mg/l) | |
|---|---|---|---|
| | | $Fe^{2+}$ | $Mn^{2+}$ |
| 10 | 45 | 0.123 | 1.69 |
| | 60 | 0.057 | 1.50 |
| | 75 | 0.046 | 1.12 |
| | 90 | 0.034 | 0.814 |
| | 105 | 0.023 | 0.71 |
| | 120 | 0.0248 | 0.911 |
| 20 | 45 | 0.101 | 1.62 |
| | 60 | 0.054 | 1.43 |
| | 75 | 0.039 | 1.0 |
| | 90 | 0.029 | 0.802 |
| | 105 | 0.02 | 0.612 |
| | 120 | 0.031 | 0.656 |
| 30 | 45 | 0.081 | 1.578 |
| | 60 | 0.044 | 1.3 |
| | 75 | 0.04 | 0.911 |
| | 90 | 0.02 | 0.572 |
| | 105 | 0.007 | 0.429 |
| | 120 | 0.019 | 0.625 |
| 40 | 45 | 0.079 | 1.497 |
| | 60 | 0.042 | 1.27 |
| | 75 | 0.021 | 0.711 |
| | 90 | 0.015 | 0.418 |
| | 105 | 0.004 | 0.321 |
| | 120 | 0.01 | 0.4 |

Based on Table 1, a graph was generated to evaluate the influence of adsorbent height and sampling time on the removal efficiency of $Fe^{2+}$ and $Mn^{2+}$ using fly ash. The $Fe^{2+}$ and $Mn^{2+}$ removal efficiency graph is presented in Figures 1 and 2.

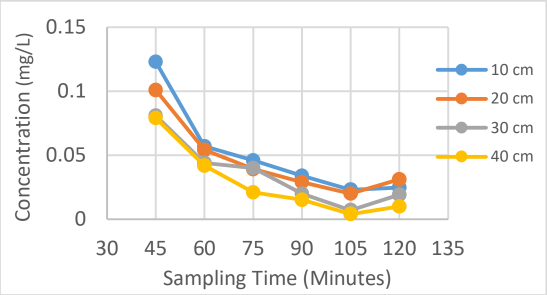

**Figure 1**. Graph of $Fe^{2+}$ Concentration Reduction using Fly Ash Adsorbent

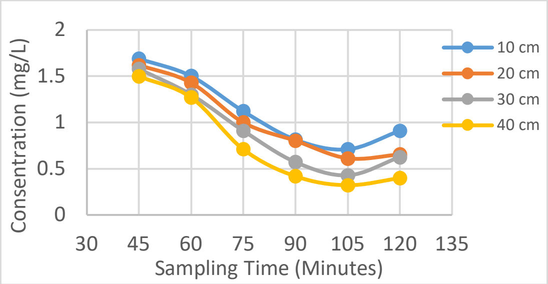

**Figure 2**. Graph of $Mn^{2+}$ Concentration Reduction using Fly Ash Adsorbent

Meanwhile, the reduction in $Fe^{2+}$ and $Mn^{2+}$ concentrations using corncob as an alternative adsorbent is presented in Table 2 below.

**Table 2**. Reduction of $Fe^{2+}$ and $Mn^{2+}$ using Corncob as an Alternative Adsorbent

| Adsorben Height (cm) | Sampling Time (minutes) | Reduction in Concentration (mg/l) | |
|---|---|---|---|
| | | $Fe^{2+}$ | $Mn^{2+}$ |
| 10 | 45 | 0.083 | 1.110 |
| | 60 | 0.064 | 0.985 |
| | 75 | 0.049 | 0.749 |
| | 90 | 0.03 | 0.580 |
| | 105 | 0.038 | 0.708 |
| | 120 | 0.051 | 0.670 |
| 20 | 45 | 0.074 | 1.053 |
| | 60 | 0.061 | 0.981 |
| | 75 | 0.04 | 0.661 |
| | 90 | 0.02 | 0.459 |
| | 105 | 0.029 | 0.498 |
| | 120 | 0.049 | 0.499 |
| 30 | 45 | 0.071 | 0.991 |
| | 60 | 0.055 | 0.852 |
| | 75 | 0.035 | 0.587 |
| | 90 | 0.017 | 0.364 |
| | 105 | 0.025 | 0.405 |
| | 120 | 0.043 | 0.528 |
| 40 | 45 | 0.066 | 1.110 |
| | 60 | 0.047 | 0.985 |
| | 75 | 0.023 | 0.749 |
| | 90 | 0.01 | 0.580 |
| | 105 | 0.014 | 0.708 |
| | 120 | 0.039 | 0.670 |

Based on Table 2, the removal efficiency graphs for $Fe^{2+}$ and $Mn^{2+}$ are presented in Figures 3 and 4.

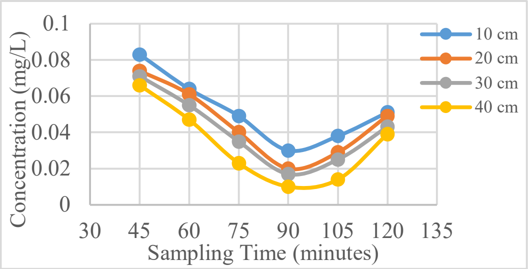

**Figure 3**. Graph of $Fe^{2+}$ Concentration Reduction using Corncob Adsorbent

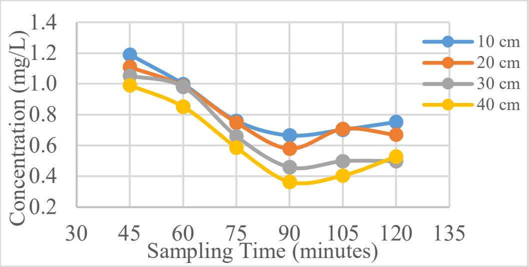

**Figure 4**. Graph of $Mn^{2+}$ Concentration Reduction using Corncob Adsorbent

Based on the analysis presented in Tables 1 and 2, both fly ash and corncob demonstrated that increasing the adsorbent bed height and sampling time significantly influenced the removal efficiency of $Fe^{2+}$ and $Mn^{2+}$ ions in groundwater. In general, higher adsorbent columns and longer contact times enhanced metal removal efficiency and reduced $Fe^{2+}$ and $Mn^{2+}$ concentrations until reaching an optimum point before adsorbent saturation. Increasing the bed height extends and stabilizes the mass transfer zone, enabling more effective diffusion of $Fe^{2+}$ and $Mn^{2+}$ ions into the pore structure of the adsorbent. This is consistent with continuous adsorption kinetics, in which mass transfer rates are governed by surface area availability and the length of the contact zone between the liquid and solid phases.

In terms of sampling time, the adsorption process exhibited an initial rapid uptake phase within the first 0–45 minutes due to the abundance of available active sites, followed by a slower phase between 90–120 minutes as most active sites became occupied and the system approached equilibrium. After exceeding the optimum time—105 minutes for fly ash and 90 minutes for corncob—a slight increase in ion concentrations was observed due to adsorbent saturation and partial desorption of ions from the surface, indicating that adsorption capacity was nearing its maximum.

For fly ash, the optimum condition was achieved at 105 minutes with a column height of 40 cm, resulting in $Fe^{2+}$ removal efficiency of 99.7% and $Mn^{2+}$ removal efficiency of 89.2%. Meanwhile, corncob reached its optimum at 90 minutes, achieving 99.2% $Fe^{2+}$ removal and 87.7% $Mn^2$ removal. These findings confirm that both materials possess promising potential as alternative adsorbents for treating groundwater contaminated with heavy metals.

The improvement in removal efficiency corresponded with the reduction in dissolved metal ion concentrations as the adsorbent bed height increased. Under optimum conditions at a height of 40 cm, fly ash reduced $Fe^{2+}$ concentrations to 0.004 mg/L, while corncob reduced them to 0.01 mg/L. $Mn^{2+}$ concentrations decreased to 0.321 mg/L with fly ash and 0.364 mg/L with corncob. According to the Indonesian Ministry of Health Regulation 2/2023, the allowable limit for $Fe^{2+}$ is 0.2 mg/L, which is already met in this study, while $Mn^{2+}$ remains slightly above the permissible limit of 0.1 mg/L. Thus, both adsorbents were effective in removing $Fe^{2+}$ but were not yet optimal for $Mn^{2+}$ reduction.

Differences in efficiency between the two adsorbents are primarily attributed to particle size and physical characteristics. Fly ash with a particle size of 200–300 mesh has a larger specific surface area than corncob (100–150 mesh). A higher surface area increases the number of active sites and reduces the diffusion distance for metal ions, thereby accelerating adsorption. The dominant mineral components of fly ash—such as silica ($SiO_2$), alumina ($Al_2O_3$), and iron oxide ($Fe_2O_3$)—also enhance adsorption through ion exchange and surface complexation mechanisms.

Conversely, corncob consists of lignocellulosic material containing functional groups such as –OH, –COOH, and $–NH_2$, which contribute to metal binding. However, its lower porosity and smaller effective surface area result in a slower adsorption process and faster saturation. A study by Yun et al., (2022) Indicated that corncob biochar has a surface area of approximately 0.50 m$^2$/g, whereas combining corncob with fly ash increases the surface area to 137 m$^2$/g, significantly improving metal removal efficiency.

Their chemical properties and valence states can explain the difference in removal efficiency between $Fe^{2+}$ and $Mn^2$. Activation using $H_3PO_4$ produces a hydrophilic surface enriched with –OH, –COOH, and $–PO_4H_2$ groups capable of interacting with positively charged ions. $Fe^{2+}$, which readily oxidizes to $Fe^{3+}$, exhibits stronger electrostatic attraction to negatively charged functional groups and tends to form $Fe(OH)_3$ precipitates on the adsorbent surface, enhancing removal through combined adsorption–precipitation mechanisms. In contrast, $Mn^{2+}$ is more stable and less prone to oxidation at neutral pH, leading to weaker interactions and lower adsorption capacity [17].

These results align with those of Susilawati et al (2023), who reported $Fe^{2+}$ removal of 92.37% and $Mn^{2+}$ removal of 53.49% using natural zeolite combined with bottom ash. Similarly, Zadeh et al., (2022) demonstrated that rice straw bioadsorbent reduced $Fe^{2+}$ by 88.59% and $Mn^{2+}$ by 86.01%. Based on these comparisons, fly ash exhibits a higher adsorption capacity than biomass-based adsorbents due to its complex pore structure and dominant mineral oxide content.

### 3.3. Shifts in Functional Groups of Alternative Adsorbents

FTIR (Fourier Transform Infrared Spectroscopy) analysis was conducted to identify changes in the active functional groups of fly ash and corncob before and after adsorption. Shifts or variations in the intensity of absorption bands indicate interactions between the adsorbent's functional groups and metal ions through hydrogen bonding, electrostatic interactions, or complex formation [20]. The FTIR spectra of fly ash are presented in Figure 5.

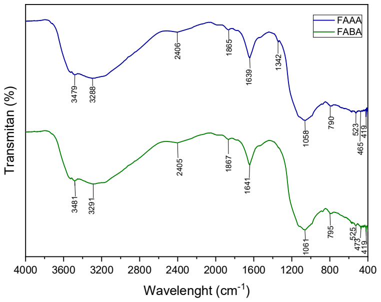

**Figure 5.** FTIR Spectrum of Fly Ash Adsorbent

Based on the FTIR analysis, the spectrum of fly ash before adsorption (FABA) exhibits major absorption bands at 3291–3481 cm$^{-1}$, corresponding to –OH groups from adsorbed water and silanol (Si–OH). After adsorption (FAAA), this band shifts to 3288–3479 cm$^{-1}$ with reduced intensity, indicating the active role of hydroxyl groups in the ion-exchange mechanism involving $Fe^{2+}$ and $Mn^{2+}$ [21]. Additional shifts occur at 1641 cm$^{-1}$ to 1639 cm$^{-1}$ and at the Si–O–Si/Si–O–Al vibration band from 1061 cm$^{-1}$ to 1058 cm$^{-1}$, reflecting interactions between silica and aluminosilicate groups with the metal ions. [22]. The absorption band originally observed at 795 cm$^{-1}$ shifts slightly to 790 cm$^{-1}$, while the lower-frequency bands in the range of 419–525 cm$^{-1}$ exhibit only minor variations, indicating that the core structure of the fly ash remains unchanged. The appearance of a new band at 1342 cm$^{-1}$ reflects the development of C–O functional groups, likely resulting from chemical interactions between metal ions and the adsorbent surface.

The FTIR spectra of the corncob adsorbent prior to and following adsorption are presented in Figure 6.

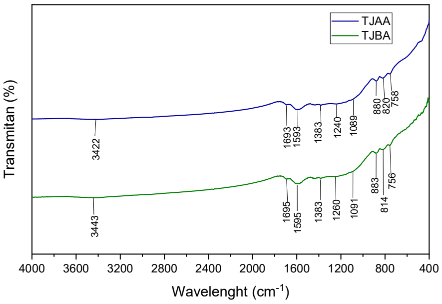

**Figure 6.** FTIR Spectrum of Corncob Adsorbent

Prior to adsorption (TJBA), the corncob spectrum displays a broad band at 3443 cm$^{-1}$, indicating the presence of –OH groups from cellulose and lignin. After adsorption (TJJA), this band shifts to 3422 cm$^{-1}$ with reduced intensity, suggesting the involvement of hydroxyl groups in hydrogen bonding with $Fe^{2+}$

and $Mn^{2+}$ ions. The carbonyl (C=O) band at 1695 cm$^{-1}$ shifts to 1693 cm$^{-1}$, reflecting interactions between the carbonyl oxygen and the metal ions. Additional shifts occur at 1595 cm$^{-1}$ to 1593 cm$^{-1}$ ($COO^-$) and at 1260 cm$^{-1}$ and 1091 cm$^{-1}$ to 1240 cm$^{-1}$ and 1089 cm$^{-1}$, indicating the participation of C–O and C–O–C groups in the adsorption process [23]. The C–H alkene band (756–883 cm$^{-1}$) shows only minor shifts, signifying physical interactions without modifications to the main structural backbone. These changes demonstrate weak interactions between alkenyl groups and the metal ions, likely through van der Waals forces or hydrogen bonding, without altering the core chemical structure of the adsorbent [24].

### 3.4. *Thomas Kinetic Model*

The Thomas isotherm model describes the relationship between the initial solute concentration ($C_0$) and the effluent concentration ($C_e$) in a continuous fixed-bed column. It assumes pseudo–first-order kinetics, negligible intraparticle diffusion, and uniform mass transfer. A linear plot of $\ln[(C_0/Ct) - 1]$ versus time (t) is used to determine $K_T$ and $Q_0$ where the slope and intercept correspond to $K_t \cdot C_0$ and $K_t \cdot Q_0 \cdot m / Q$, respectively. The calculated Thomas parameters are summarized in Table 3 and Table 4.

**Table 3**. Thomas Kinetic Model using Fly Ash Adsorbent

| Parameter | Adsorbent Height (cm) | $K_T$ (mL/mg.min) | $Q_0$ (mg/g) | Qe (mg/g) |
|---|---|---|---|---|
| $Fe^{2+}$ | 10 | 0.179 | 0.029 | 0.025 |
| | 20 | 0.243 | 0.017 | 0.013 |
| | 30 | 0.295 | 0.011 | 0.009 |
| | 40 | 0.318 | 0.008 | 0.006 |
| $Mn^{2+}$ | 10 | 0.108 | 0.053 | 0.035 |
| | 20 | 0.109 | 0.031 | 0.019 |
| | 30 | 0.122 | 0.020 | 0.013 |
| | 40 | 0.130 | 0.016 | 0.010 |

**Table 4**. Thomas Kinetic Model using Corncob Adsorbent

| Parameter | Adsorbent Height (cm) | $K_T$ (mL/mg.min) | $Q_0$ (mg/g) | Qe (mg/g) |
|---|---|---|---|---|
| $Fe^{2+}$ | 10 | 0.097 | 0.091 | 0.068 |
| | 20 | 0.143 | 0.047 | 0.034 |
| | 30 | 0.177 | 0.026 | 0.023 |
| | 40 | 0.194 | 0.023 | 0.017 |
| $Mn^{2+}$ | 10 | 0.137 | 0.130 | 0.111 |
| | 20 | 0.140 | 0.069 | 0.057 |
| | 30 | 0.153 | 0.054 | 0.040 |
| | 40 | 0.189 | 0.035 | 0.031 |

The theoretical adsorption capacity ($Q_0$) shows a decreasing trend with increasing bed height, even though a larger amount of adsorbent is used. This decline is attributed to a reduced ratio of the volume of solution passing through the column to the number of active sites participating in the adsorption process. At greater bed heights, most metal ions are captured in the upper section of the column, resulting in lower ion concentrations reaching the lower layers, which prevents them from achieving equilibrium within the same operational period. According to the Mass Transfer Zone (MTZ) concept, increasing column height extends the MTZ, leading to a lower specific capacity ($Q_e$) despite an overall increase in total system capacity.

Corncob adsorbent exhibits higher $Q_0$ values compared to fly ash for both $Fe^{2+}$ and $Mn^{2+}$. This difference is associated with the more porous surface structure of corncob and the presence of active functional groups such as –OH and –COOH, which facilitate stronger interactions with metal ions. In contrast, fly ash possesses an inorganic mineral structure with a relatively smaller specific surface area and a predominance of Si–O–Al bonds, limiting its interaction capacity with metal ions. Furthermore, $Fe^{2+}$ demonstrates a higher adsorption capacity than $Mn^{2+}$ due to differences in ionic radius and chemical affinity toward the active sites on both adsorbents.

The adsorption rate constant ($K_T$) increases with higher bed height, indicating enhanced mass transfer efficiency due to longer contact time and greater interaction surface area. In taller columns, both external and internal diffusion processes occur more effectively, thereby accelerating the pseudo–first-order kinetics of adsorption. Fly ash exhibits the highest $K_T$ values for $Fe^{2+}$, indicating faster adsorption kinetics attributed to its smoother surface and more uniform pore distribution. In contrast, corncob shows a steadier increase in $K_T$ dominated by internal diffusion mechanisms. Overall, increasing bed height expands the effective adsorption zone and accelerates adsorption kinetics, contributing to higher metal ion removal efficiency in continuous-column systems.

The coefficient of determination ($R^2$) confirms strong agreement between the experimental data and the Thomas model, ranging from 0.9096–0.9764 for $Fe^{2+}$ on fly ash, 0.8554–0.8730 for $Mn^{2+}$ on fly ash, 0.8052–0.8370 for $Fe^{2+}$ on corncob, and 0.9380–0.9807 for $Mn^{2+}$ on corncob. These results demonstrate that the Thomas model provides a theoretically appropriate representation of the adsorption kinetics of $Fe^{2+}$ and $Mn^{2+}$ for both types of adsorbents.

## 4. CONCLUSION

The findings indicate that both fly ash and corncob are effective alternative adsorbents for removing $Fe^{2+}$ and $Mn^{2+}$ ions from groundwater. Under optimal conditions, fly ash achieved removal efficiencies of 99.7% for $Fe^{2+}$ and 89.2% for $Mn^{2+}$, while corncob achieved 99.2% for $Fe^{2+}$ and 87.7% for $Mn^{2+}$. Increasing the adsorbent bed height and contact time enhanced adsorption efficiency, with optimal contact times of 105 minutes for fly ash and 90 minutes for corncob. FTIR analysis demonstrated that the active functional groups, such as –OH, Si–O, and C–O, on fly ash, as well as –OH, C=O, and C–O on corncob, participated in the adsorption process, indicating chemical interactions between the metal ions and the surfaces of the adsorbents. The Thomas model effectively captured the adsorption behavior, showing that $Q_0$ declined as bed height increased, while KT rose, indicating improved mass transfer efficiency. Overall, corncob exhibited higher adsorption capacity, while fly ash demonstrated faster

https://doi.org/10.29165/ajarcde.v10i3.836

kinetic performance. The coefficient of determination ($R^2$ = 0.8052–0.9807) confirms that the Thomas model provides an excellent prediction of metal-ion adsorption behaviour in continuous column systems, supporting the potential application of both adsorbents for sustainable groundwater treatment.

## REFERENCE

[1] Y. H. Dulanlebit, Sunarti, and Y. T. Male, "Efektivitas Biji Kelor (Moringa Oleifera Lamk) Pada Pengolahan Air Sumur dan Penentuan Waktu Optimum Adsorpsi Biji Kelor Terhadap Fe dan Mg Dalam Air," *Molluca J. Chem. Educ.*, vol. 10, no. 1, pp. 43–52, 2020, doi: 10.30598/mjocevol10iss1pp43-52.

[2] I. F. Anggraini, E. Kusniawati, and M. Mayangsari, "Pemanfaatan Tongkol Jagung pada Pembuatan Karbon Aktif dengan Mneggunakan Aktivator Na2CO3 serta Pengaruhnya terhadap Sampel Air Sumur Gali Menggunakkan Parameter pH, Turbidity, TSS, dan TDS," *J. Cakrawala Ilm.*, vol. 2, no. 5, pp. 2261–2272, 2023.

[3] R. A. F. Lubis, H. I. Nasution, and M. Zubir, "Production of Activated Carbon from Natural Sources for Water Purification," *Indones. J. Chem. Sci. Technol.*, vol. 3, no. 2, p. 67, 2020, doi: 10.24114/ijcst.v3i2.19531.

[4] D. G. Purwitasari, R. Tussania, and R. Fathoni, "Adsorpsi Logam Kadmium (Cd) Pada Kadmium Sulfat (Cdso4) Menggunakan Batang Pohon Pisang sebagai Adsorben," *J. Chemurg.*, vol. 6, no. 1, p. 52, 2022, doi: 10.30872/cmg.v6i1.7905.

[5] Joko Murtono and Iriany, "Pembuatan Karbon Aktif dari Cangkang Buah Karet dengan Aktivator H3PO¬4 dan Aplikasi sebagai Penjerap Pb(II)," *J. Tek. Kim. USU*, vol. 6, no. 1, pp. 43–48, 2017, doi: 10.32734/jtk.v6i1.1564.

[6] E. Sulistyawati, W. W. Nandari, A. R. Nurchasanah, and K. K. Dewi, "Kinetika Adsorpsi Mikrokapsul Kitosan Taut Silang Kalium Persulfat terhadap Zat Warna Methyl Orange," *J. Rekayasa Proses*, vol. 14, no. 1, pp. 47–59, 2020, doi: 10.22146/jrekpros.50634.

[7] M. Setiawati, "Fly Ash sebagai Bahan Pengganti Semen Pada Beton," *Semin. Nas. Sains dan Teknol. 2018*, vol. 5, no. 4, pp. 295–302, 2018.

[8] D. Ambia, "Pemanfaatan Fly Ash Batubara sebagai Adsorben pada Peyerapan Polutan di Pengolahan Air Lindi TPA Blang Bintang Aceh Besar," Universitas Islan Negeri Ar-Raniry, 2021.

[9] A. P. Wardani, S. D. Maulidz, and ..., "Pemanfaatan Fly Ash sebagai Material Adsorben untuk Menurunkan Kandungan Logam Fe pada Limbah Cair di Unit Waste Water Treatment Plant PT POMI," *Distilat J. ...*, 2021, [Online]. Available: https://pdfs.semanticscholar.org/e59c/8f0d01bae10fe387f48ad1e8e5d10b5690df.pdf

[10] A. A. Kusuma, B. Lathifaturrohmah, and E. E. Dyah Lestari, "Pengaruh Penambahan Arang Aktif Limbah Tongkol Jagung untuk Mengurangi Kadar Kesadahan Total," *Walisongo J. Chem.*, vol. 3, no. 1, p. 31, 2020, doi: 10.21580/wjc.v3i1.6128.

[11] M. Ganing, "Pengaruh Konsentrasi Aktivator NaOH pada Arang Aktif Tongkol Jagung terhadap Adsorpsi Ion Pb2+," *J. Teknol. Kim. Miner.*, vol. 1, no. 2, pp. 76–80, 2022, doi: 10.61844/jtkm.v1i2.265.

[12] S. Harmawanda, D. Wahyuni, M. Nurhanisa, Hasanuddin, and Zulfian, "Efektivitas Karbon Aktif dari Limbah Tongkol Jagung (Zea mays) dengan Variasi Aktivator Asam Klorida dalam Penyerapan Logam Besi pada Air Gambut," *J. Fis.*, vol. 13, no. 1, pp. 10–19, 2023, doi: 10.15294/jf.v13i1.42778.

[13] I. Syafrianda, E. Yenie, and S. Daud, "Pengaruh Waktu Kontak dan Laju Pengadukan Terhadap Adsorpsi Zat Warna Pada Air Gambut Menggunakan Adsorben Limbah Biosolid Land Application Industri Minyak Kelapa Sawit," *J. Online Mhs. Fak. Tek. Univ. Riau*, vol. 4, no. 2, pp. 1–6, 2017.

[14] A. S. Reyra, S. Daud, and S. R. Yenti, "Pengaruh Massa dan Ukuran Partikel Adsorben Daun Nanas Terhadap Efisiensi Penyisihan Fe Pada Air Gambut," *J. Online Mhs. Fak. Tek. Univ. Riau*, vol. 4, no. 2, pp. 1–9, 2017.

[15] M. H. Marzbali and M. Esmaieli, "View of Fixed Bed Adsorption of Tetracycline on a Mesoporous Activated Carbon: Experimental Study and Neuro-Fuzzy Modelling," *J. Appl. Res. Technol.*, vol. 15, pp. 454–463, 2017, [Online]. Available: https://doi.org/10.1016/j.jart.2017.05.003

[16] X. Yun, Y. Ma, H. Zheng, Y. Zhang, B. Cui, and B. Xing, "Pb(II) Adsorption by Biochar from Co-Pyrolysis of Corn Stalks and Alkali-Fused Fly Ash," *Biochar*, vol. 4, no. 1, 2022, doi: 10.1007/s42773-022-00189-4.

[17] U. O. Aigbe, K. E. Ukhurebor, R. B. Onyancha, O. A. Osibote, H. Darmokoesoemo, and H. S. Kusuma, "Fly Ash-Based Adsorbent for Adsorption of Heavy Metals and Dyes from Aqueous Solution: A Review," *J. Mater. Res. Technol.*, vol. 14, pp. 2751–2774, 2021, doi: 10.1016/j.jmrt.2021.07.140.

[18] S. Susilawati, N. S. Lubis, and K. M. Pasaribu, "The Synthesis and Characterization of Pahae Natural Zeolite-Coal Bottom Ash Adsorbent for Fe and Mn Purifier in Well Water," *J. Kim. Sains dan Apl.*, vol. 26, no. 6, pp. 211–216, 2023, doi: 10.14710/jksa.26.6.211-216.

[19] M. A. Zadeh, A. Daghbandan, and B. Abbasi Souraki, "Removal of Iron and Manganese from Groundwater Sources Using Nano-Biosorbents," *Chem. Biol. Technol. Agric.*, vol. 9, no. 1, pp. 1–14, 2022, doi: 10.1186/s40538-021-00268-x.

[20] J. M. Munene, J. O. Onyatta, and A. O. Yusuf, "Characterization of Water Hyacinth Powder Using FTIR Spectroscopy and the Adsorption Behaviour of Pb2+, Cd2+, Zn2+, Ni2+ and Cr2+ in Aqueous Solution," *Asian J. Appl. Chem. Res.*, vol. 6, no. 1, pp. 47–55, 2020, doi: 10.9734/ajacr/2020/v6i130151.

[21] K. R. K. D. Sangandita and B. Utami, "Efektivitas Sekam Padi dan Bagasse Fly Ash sebagai Adsorben Logam Cr pada Sistem batch," *JKPK (Jurnal Kim. dan Pendidik. Kim.*, vol. 4, no. 2, p. 85, 2019, doi: 10.20961/jkpk.v4i2.29724.

[22] L. Panda and S. Dash, "Characterization and Utilization of Coal Fly Ash: A Review," *Emerg. Mater. Res.*, vol. 9, no. 3, pp. 921–934, 2020, doi: 10.1680/jemmr.18.00097.

[23] M. K. Rafiq, R. T. Bachmann, M. T. Rafiq, Z. Shang, S. Joseph, and R. L. Long, "Influence of Pyrolysis Temperature on Physico-Chemical Properties of Corn Stover (Zea Mays l.) Biochar and Feasibility for Carbon Capture and Energy Balance," *PLoS One*, vol. 11, no. 6, pp. 1–17, 2016, doi: 10.1371/journal.pone.0156894.

[24] D. A. Hartanto, P. E. Yuwita, and R. N. Faila, "Karakterisasi Gugus Fungsi pada Karbon Aktif Kulit Jagung Menggunakan Uji Fourier Transform Infrared sebagai Bahan Pembuatan Adsorben," *Invent. (Journal Sci. Technol.*, vol. 4, no. 1, pp. 1–9, 2023.